INTER-CALIBRATION OF METEOSAT IMAGERS AND IASI

Tim J. Hewison and Marianne König

EUMETSAT, Am Kavalleriesand 31, 64295 Darmstadt, Germany

Abstract

EUMETSAT has initiated routine inter-calibration of the infrared channels of Meteosat imagers and the Infrared Atmospheric Sounding Interferometer (IASI) on Metop-A, based on the regression of collocated radiance observations, weighted according to their spatial variability. This paper describes the algorithm and presents key results for Meteosat-7, -8 and -9 during 2007. These demonstrate the reliability of the inter-calibration method and show it can be used to monitor the gradual change in calibration bias of the 13.4 µm channel of Meteosat-9. This is shown to be consistent with the build up of ice contamination on the instrument's optical elements and can be reduced by performing periodic decontamination processes – warming the instrument's optics to drive off condensates. The modelling of this process, together with the inter-calibration monitoring can help understand the mechanism responsible for the changing biases and develop and validate operational corrections.

INTRODUCTION

This paper describes the method of performing routine comparisons between pairs of collocated observations from instruments with similar characteristics to inter-calibrate them. Initially this work has concentrated on the infrared channels of the geostationary Meteosat imagers and the Infrared Atmospheric Sounding Interferometer (IASI) on Metop-A, for which key results will be presented.

These direct comparisons of collocated observations from pairs of instruments with similar characteristics form part of EUMETSAT's inter-calibration strategy to ensure consistency amongst its products and between these and those of other operation meteorological satellites. This requires international coordination, which is achieved through the Global Space-based Inter-Calibration System (GSICS). Another approach being investigated in parallel is the analysis of observation biases with respect to forward-modelled Numerical Weather Prediction (NWP) model fields. Such *double-differencing* methods allow indirect comparison of different observations over a broader range of conditions than may be achieved by direct comparisons. In this way any biases from the NWP or associated radiative transfer model will be minimised when comparing the relative biases for two instruments.

In this work IASI has been adopted as a *de facto* reference standard, as agreed by GSICS, because it is well-specified, provides contiguous spectral coverage of the band of Meteosat's infrared channels, includes built-in calibration and non-linearity controls and has undergone careful pre-launch characterisation (Blumstein *et al*., 2004) and post-launch validation (Smith *et al.,* 2008). Other inter-calibration work has used the Atmospheric InfraRed Sounder (AIRS) on the Aqua polar-orbiting satellite as a reference (e.g. Tahara, 2008). Although AIRS has similar advantages to IASI, it has some bad channels and gaps in its spectral coverage, which need to be accounted for and increase the uncertainty in the inter-comparisons. As AIRS and IASI are being used as reference instruments in different GSICS studies, it is important to investigate their relative inter-calibration. This can be done by analysis of Simultaneous Nadir Overpasses (Tobin, 2008).

INTER-CALIBRATION METHOD

König (2007) reported the use of IASI to simulate radiances observed by Meteosat Second Generation (MSG) SEVIRI instruments. This has been extended to include uncertainty estimation and now covers Meteosat-7, -8 and -9 for most of 2007. The method is based on comparison of collocated observations from instrument pairs during Simultaneous near-Nadir Overpasses of their satellites.

Collocation Criteria

The following collocation criteria, based on those recommended by GSICS (2007), were used to minimise the differences in the observation parameters between the two systems under comparison:

a) Time difference between observations less than Meteosat's repeat cycle.
b) The surface incidence angle from IASI to be no more than 15° from zenith.
c) The surface incidence angle from both instruments to be within 2°.
d) Only night-time data is used to minimise the effect of solar radiation on the short-wave channels.

The frequent nature of the collocations provided by comparing instruments on polar-orbiting satellites with those in geostationary orbits allows a sufficient number of pixels (~400/day) to be compared to reduce the contribution from radiometric noise to the error budget to insignificant levels even with relatively strict criteria. This method allows the relative bias between the instruments to be established in baseline conditions against which its sensitivity to the observation parameters could be compared.

Spectral Convolution

The radiance spectrum measured by IASI, *L(v)*, for each iFoV is convolved with the Spectral Response Function (SRF) of each SEVIRI channel, *r*(v) (interpolated onto a 0.25 cm^{-1} grid) to allow direct comparison of their radiances:

$$L_j = \frac{\int r_j(v) L(v) dv}{\int r_j(v) dv} \qquad (1)$$

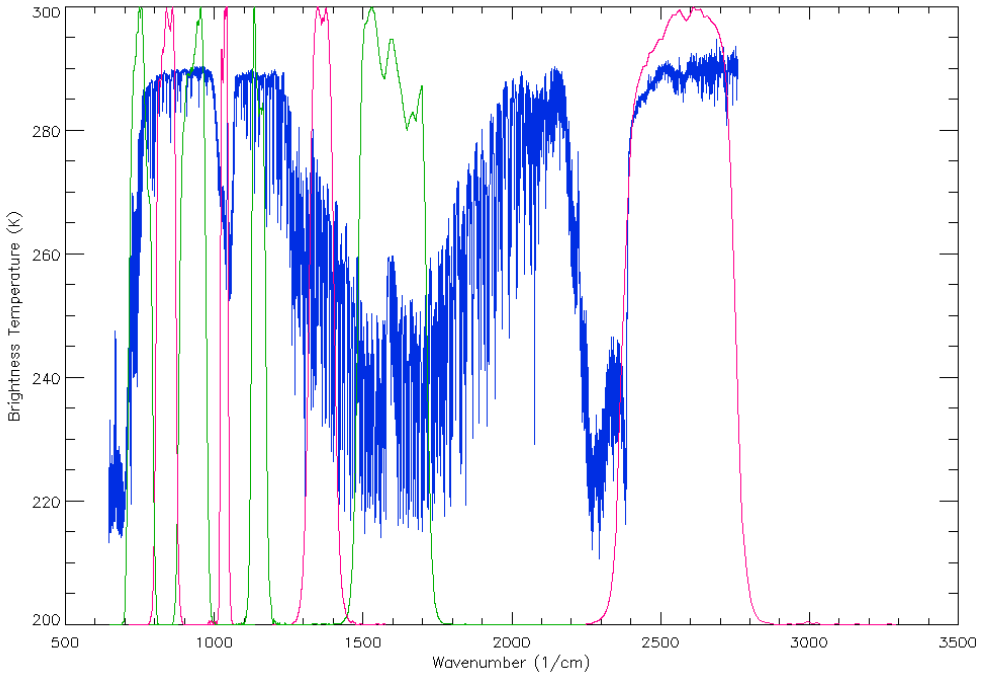

Figure 1: **Example radiance spectra measured by IASI (blue), expressed in brightness temperature (K) and Spectral Response Functions of SEVIRI channels 3-11 from right to left (red/green).**

As shown in Figure 1, the IASI spectra do not quite cover the full SRF of Meteosat's IR3.9 channel (IASI stops at 2760 cm^{-1}). This has not been accounted for in this analysis as it represents a small contribution to the total energy seen by the IR3.9 channel. The bias introduced by this approximation has been estimated as equivalent to a -0.09 K bias on a black-body at 240 K (typical cloudy scene), increasing to -0.17 K for a 290 K scene (typical clear sky).

Spatial Averaging

To ensure both instruments sample comparable spatial scales, the Meteosat pixels within the nominal area of each IASI iFoV are averaged. The variances of these pixels' radiances are also calculated to estimate the uncertainty due to spatial variability. For Meteosat-7, 3x3 pixels are used; while 5x5 pixels are used for Meteosat-8 and -9.

Weighted Regression

Comparison between Meteosat and IASI radiances is achieved by performing weighted linear regressions between all collocated radiances within each Metop overpass. The inverse of the variance of the Meteosat radiances within each IASI iFoV, σL_{IASI}^{-2}, is used as the weighting to represent the uncertainty in the collocation due to spatial variability. Examples of the linear regression for the water vapour and thermal infrared bands of Meteosat-7 are shown in Figure 2.

The linear regression yields estimates of the slope and offset of the relationship between the Meteosat and IASI radiances. The regression also estimates the uncertainty on these coefficients as the standard errors, σa_0 and σa_1. However, because they are correlated, their covariance, cov(a_0, a_1), is also needed to estimate the uncertainty, σL_{MET}, when the coefficients are applied to estimate the Meteosat radiance, L_{MET}, for a given IASI scene radiance, L_{REF} :

$$\hat{L}_{MET} = a_0 + a_1 L_{REF} \tag{2}$$

$$\sigma\hat{L}_{MET}^{\,2} = \left[\sigma a_0^{\,2} + 2\,\mathrm{cov}(a_0, a_1) L_{REF} + \sigma a_1^{\,2} L_{REF}^{\,2}\right] \tag{3}$$

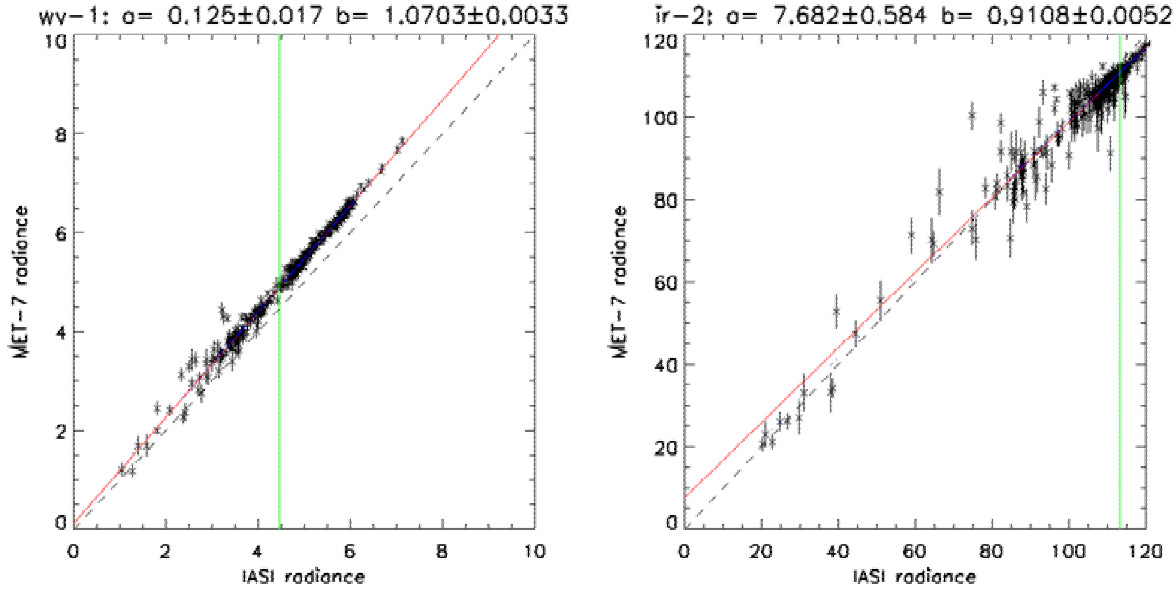

Figure 2: **Example of linear regression between collocated Meteosat-7 radiances and IASI radiance spectra convolved with the Spectral Response Functions of Meteosat. The water vapour band is shown in the left panel and the thermal infrared on the right. The units on all axes are $mW.m^{-2}.sr^{-1}.(cm^{-1})^{-1}$. Collocated radiances with low relative spatial variance (σL_{MET} <0.05 L_{REF}) are shown as points with error bars corresponding to the standard deviation of the Meteosat radiances within each IASI field of View. The weighted least square fit is shown by the red lines and the reference scene radiance by the green vertical line, for which the relative bias is calculated.**

Typical uncertainties were found to be ~0.02 K for brightness temperatures in the thermal infrared channels corresponding to tropical clear-sky scenes. However, these are believed to be underestimated due to neglecting the temporal variability. The greater day-to-day variability that was observed (~0.05 K) is believed to be due to this short-term variability.

In this analysis, the collocations were not explicitly filtered, as has been suggested (e.g. GSICS, 2007) as a method to reduce uncertainty due to scene variability. Instead, the weighted regression method relies on the higher variance of inhomogeneous scenes to reduce their influence on the results, while producing results over the full range of observed radiances. This approach has been validated by comparing the relative bias between the instruments calculated using different filtering approaches. The results for clear sky scenes were found to be independent of how the collocations were filtered.

Reference Scene Radiances

Because the slope of these regressions is not generally equal to 1, the relative bias between the instruments will depend on the scene radiance. So to facilitate comparisons, reference scene radiances, L_{REF}, have been derived for typical clear-sky scenes within the domain of the inter-comparison, as shown in Table 1. These were calculated as the modal values of the brightness temperature distribution of all pixels meeting the collocation criteria, binned to the nearest 5 K.

The reference scene radiances have been derived for typical clear-sky scenes within the domain of the inter-comparison, as shown in Table 1. These statistics were found to be independent of the method of filtering the data. This validates the decision not to filter the data. As the difference between the instruments can depend on scene radiance, the regression method has also been applied to estimate the mean difference for cloudy scenes with lower radiances (T_b=200 K). However, the results were found to be highly variable for most channels.

INTER-CALIBRATION RESULTS

Table 1 summarises the results of the inter-calibration as the mean brightness temperature differences (and their uncertainties) evaluated for the clear-sky reference scenes of all the infrared channels of Meteosat-7, -8 and -9 during 2007. The *water vapour* and *infrared* channels of Meteosat-7 both showed relatively large biases with respect to IASI (although with opposite signs). However, as is also seen in Figure 3, both channels were quite stable, with standard deviations of <0.2 K over the whole year.

The results for Meteosat-8 and -9 are consistent with those of König (2007) despite the different method: showing a large bias in the 13.4 µm channel of Meteosat-9, which was the operational geostationary satellite at 0° longitude for most of this period. The time series in Figure 5 show the biases in this and the 3.9 µm channel changed steadily during 2007, followed by a sudden recovery during the decontamination procedure of 3-11 December. The biases in the other channels remained constant, with small standard deviations ~0.05 K, were similar to those found for Meteosat-8.

Channel (µm)		3.9[¶]	6.2	7.3	8.7	9.7	10.8	12.0	13.4
Ref Scene T_{bref} (K)		290	240	260	290	270	290	290	270
Meteosat-7	Mean Bias (K)	-	**+2.57**		-	-	**-1.63**		-
	Std. Dev. (K)	-	0.12		-	-	0.19		-
Meteosat-8	Mean Bias (K)	**0.46**	**0.56**	**0.77**	**0.22**	0.19	**0.16**	0.13	-0.13
	Std. Dev. (K)	0.09	0.08	0.18	0.09	0.14	0.07	0.07	0.16
Meteosat-9	Mean Bias (K)	0.17	**0.61**	**0.25**	0.02	0.00	0.03	0.05	**-1.63**
	Std. Dev. (K)	0.10	0.05	0.04	0.04	0.07	0.06	0.06	0.26

Table 1: **Brightness Temperatures, T_b, for reference scenes and mean difference between Meteosat-IASI during 2007.**
[¶] IASI response is limited to 2760 cm^{-1}, which underestimates radiance of a 290 K scene in 3.9 µm channel by 0.17 K.

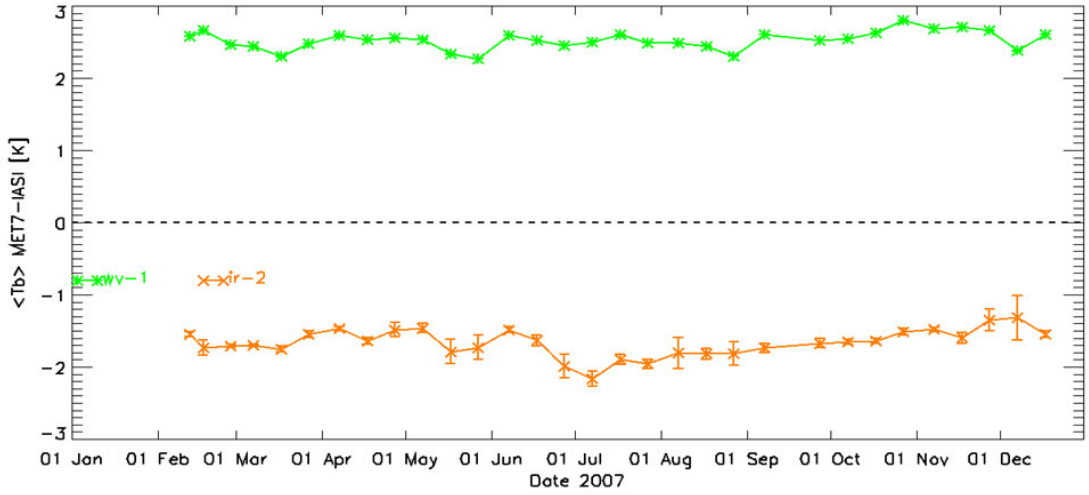

Figure 3: **Time series of brightness temperature differences between Meteosat-7-IASI for Reference Scene radiances. Each Meteosat infrared channel is shown in a different colour, with different symbols, following the legend. Error bars represent statistical uncertainty on each mean bias (may be very small).**

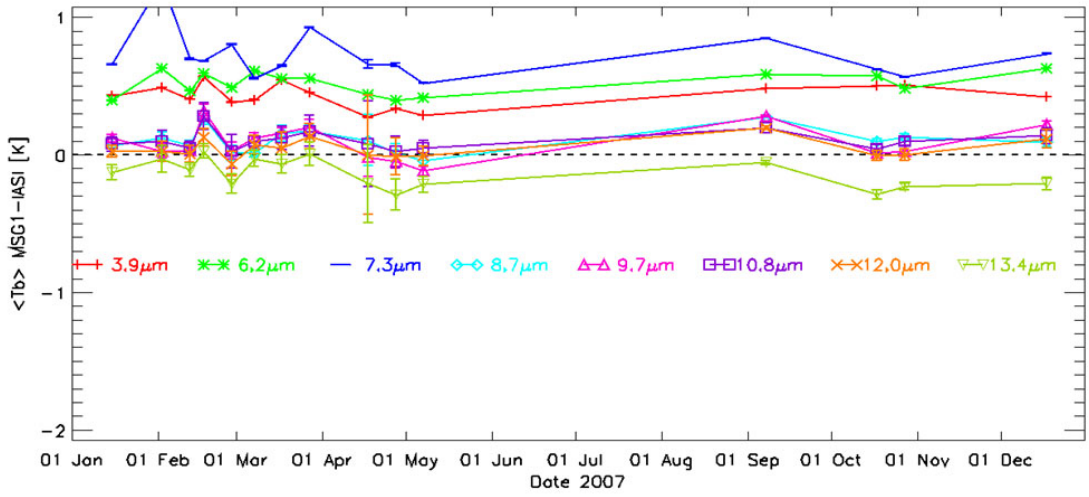

Figure 4: **As above, but for Meteosat-8 (MSG1)**

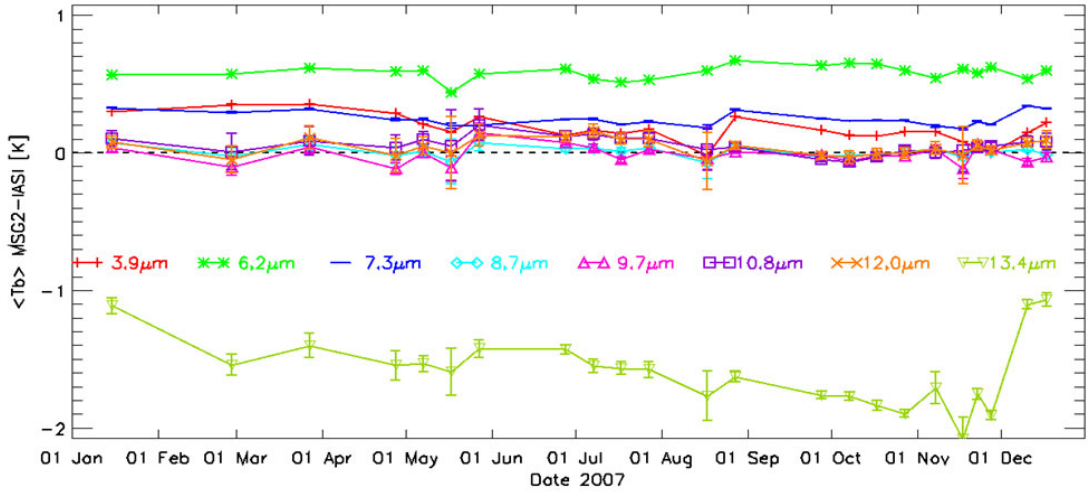

Figure 5: **As above, but for Meteosat-9 (MSG2)**

All Meteosat biases show slow variations, which may be modelled using a Kalman Filter based on inter-calibration with IASI on a ~weekly basis.

Radiance Definition

In this analysis, the *spectral* radiance definition used operationally at EUMETSAT until April 2008 (EUMETSAT, 2007) was applied to the MSG data to convert observed radiances to brightness temperatures. These were then converted to *effective* radiances, accounting for the Spectral Response Function (SRF) of each channel, for comparison with IASI radiances. Radiances from Meteosat-7 were defined in a different way, and were simply divided by the integral of each channel's SRF to convert to effective radiance.

Selected MSG cases were re-processed using the new ECP833 processing package (EUMETSAT, 2007), which included the *effective* radiance definition. (In these cases, no intermediate conversion to brightness temperatures was necessary.) As the radiance definition was correctly interpreted in the previous analysis, its change is not expected to affect the results. However, other changes were also introduced in ECP833, including changes in treatment of the black body calibration target and the non-linearity corrections. These result in slightly different relative biases – typically reducing the positive biases in the IR3.9, IR6.2 and IR7.3 channels by ~0.2 K, ~0.7 K and ~0.2 K, respectively, for both Meteosat-8 and -9, and reducing the positive bias in the IR13.4 channel of Meteosat-9 by ~0.3 K. These changes are likely to reduce the biases in all channels when operationally implemented.

ICE CONTAMINATION MODEL

These inter-calibration results can be used to test the hypothesis that the changes in biases are due to water ice condensing on the surfaces of the cold optics after outgassing from other material on the satellite. Differential absorption by this ice layer would modify the instrument's spectral response function (SRF). Although much of this would be accounted for in the internal black body calibration, signals from channels in atmospheric absorption bands could remain biased. However, since the rates of outgassing and condensation are unknown, it is not possible to estimate the ice thickness on purely theoretic grounds.

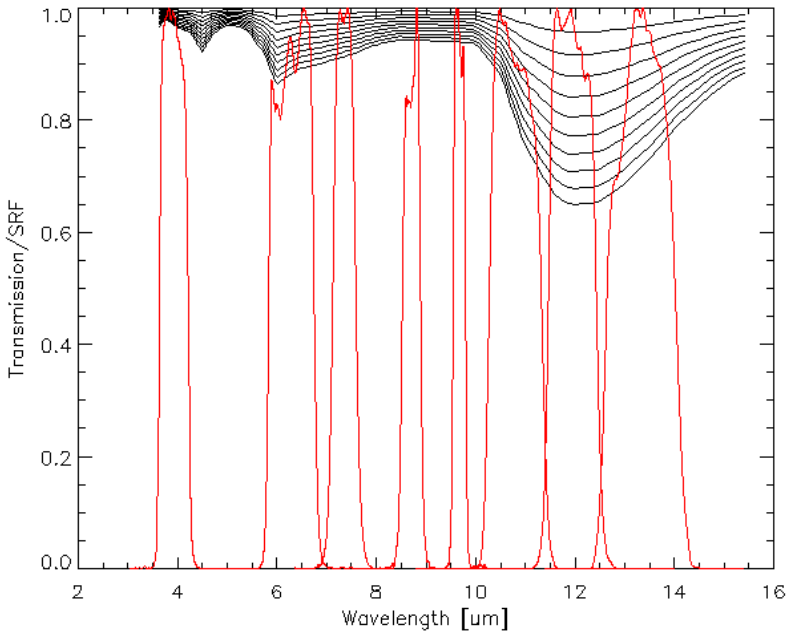

Figure 6: Transmission spectra of ice layers of different thicknesses (black): 0.1, 0.2, 0.3, 0.4, 0.5, 0.6, 0.7, 0.8, 0.9, 1.0 µm layers. Spectral Response Functions of Meteosat-8 infrared channels (red).

An ice absorption model (Warren, 1984) was used to calculate the transmission of ice layers of a range of thicknesses. This model has compared very well with IASI measurements for a range of ice thicknesses from 12 nm to 3.7 μm (D.Blumstein, personal communication, 12/03/08), except for the short wavelength range (<4 μm). The modelled transmissions for 10 different ice thicknesses are plotted together in Figure 6, which also shows the SRFs of the infrared channels on Meteosat-8 (MSG1).

Radiances were simulated by convolving a typical radiance spectrum observed by IASI in clear sky with MSG SRFs – initially unperturbed, then modifying the SRFs by convolving them with the transmission spectra for various ice thicknesses. This was repeated for the black body calibration reference to establish the change in gain expected. Finally, the expected brightness temperatures were calculated for each MSG channel and compared with those using the original, unperturbed, SRFs.

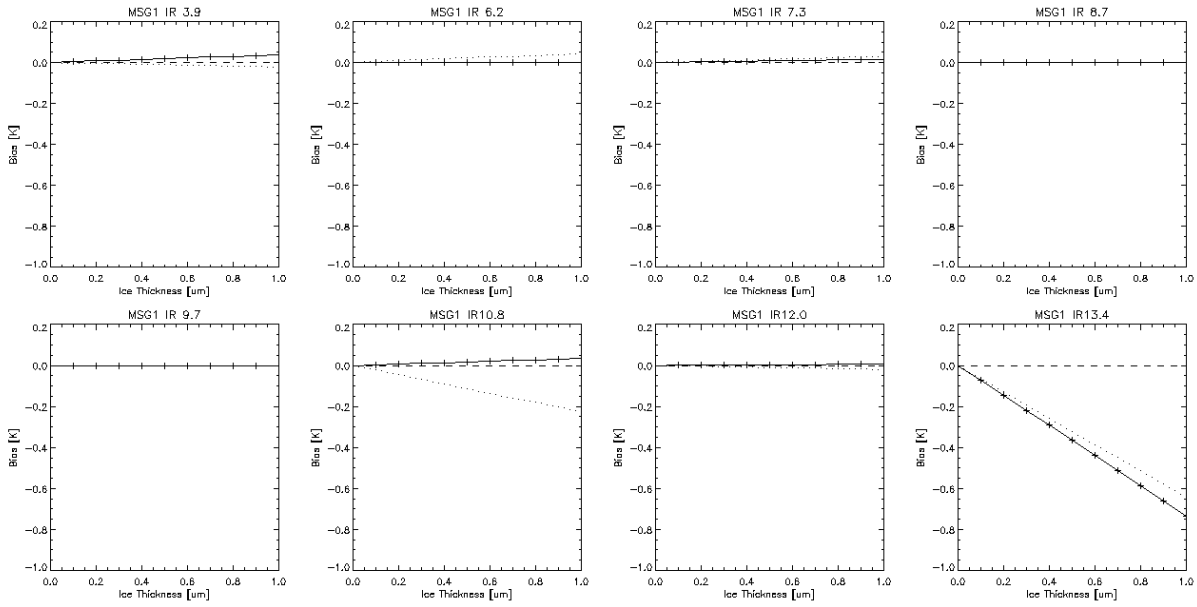

Figure 7: Bias in brightness temperatures modelled by modifying the SRFs of Meteosat-8 (MSG1) by the transmission of different thicknesses of ice, following the model described above. Solid line with crosses shows the predicted differences in brightness temperature compared with the uncontaminated instrument, accounting for calibration gain changes. The dotted line shows the result without accounting for these gain changes.

The brightness temperature biases modelled in this way for each MSG channel are plotted in Figure 7 as a function of ice thickness. These predictions closely resemble the observed biases for Meteosat-9 in Figure 5. i.e. The IR13.4 channel shows a bias that changed at a rate of -0.7 K/yr, while other channels remained relatively unaffected by ice contamination. These results are consistent with the gradual build-up of a layer of ice ~1 μm thick over the year. This ice layer was removed by heating the optics during the decontamination process, after which the biases returned to their nominal values.

Channel	Feb-2006	d /μm	Jun-2006	d /μm	Dec-2006	d /μm	Dec-2007	d /μm
IR3.9	6%	0.5	6%	0.5	6%	0.5	6%	0.5
IR6.2	21%	1.3	8%	0.5	6%	0.4	10%	0.6
IR7.3	13%	1.0	4%	0.3	3%	0.3	6%	0.5
IR8.7	8%	1.0	6%	0.8	4%	0.5	6%	0.7
IR9.7	6%	0.7	1%	0.2	1%	0.1	2%	0.3
IR10.8	44%	1.7	22%	0.9	14%	0.6	23%	1.0
IR12.0	115%	1.6	49%	0.8	34%	0.6	50%	0.8
IR13.4	66%	1.2	27%	0.5	23%	0.4	30%	0.6

Table 2: **Gain Changes (%) in Meteosat-9 IR channels during decontaminations and ice thickness (μm) estimated from these using the ice transmission model.**

This theory is further supported by the independent observation that the gains of the infrared channels changed during the decontamination procedure in a way consistent with transmission losses of an ice layer ~0.8 mm thick, as shown in Table 2. It would, therefore, be possible to develop a physically-based algorithm to correct these biases by using the observed gain changes to estimate the thickness of the contaminating ice layer.

CONCLUSIONS

Within the framework of GSICS, a method has been developed to inter-calibrate the infrared channels of Meteosat sensors using the Infrared Atmospheric Sounding Interferometer (IASI) on Metop-A, based on the regression of collocated radiance observations, weighted according to their spatial variability. This method has been shown to produce reliable results with low uncertainties and provides the capability of monitoring changes in the relative calibration of the instruments. Furthermore, the inter-calibration datasets have allowed the testing of a hypothetical bias mechanism affecting the IR13.4 channel of Meteosat-9 and the development of operational corrections.

STOP PRESS

Since writing this paper, a mistake has been found in the spectral response function (SRF) used in the IR13.4 channel of Meteosat-9. When the correct SRF is used, the relative biases of selected cases were found to be ~0.2 K less negative, although it remained significantly biased and subject to drift at the same rate described herein. Other channels are not affected.

REFERENCES

Blumstein, D., *et al.,* (2004) IASI instrument: Technical overview and measured performances, SPIE Conference, Denver (Co), August 2004, **SPIE** 2004-5543-22

EUMETSAT, (2007) A Planned Change to the MSG Level 1.5 Image Product Radiance Definition, **EUMETSAT Document** EUM/OPS-MSG/TEN/06/0519 Available online from http://www.eumetsat.int.

GSICS, (2007) GRWG GEO-AIRS Inter-calibration Algorithm 1.0, Unpublished.

Hewison, T. J. (2008) The Inter-calibration of Meteosat and IASI during 2007, **EUMETSAT Technical Report** EUM/MET/REP/08/0052, April 2008. Available from http://www.eumetsat.int.

König, M., (2007) Inter-calibration of IASI with MSG-1/2 onboard METEOSAT-9, **GSICS Quarterly**, Vol.1, No.2.

Smith, W., *et al.*, (2008) Joint Airborne IASI Validation Experiment (JAIVEx) - An overview, **Proc. Int. ATOVS Study Conf.** XVI, Angra dos Reis, Brazil, CIMSS, University of Wisconsin–Madison, in press.

Tahara, Y., K. Kato, A. Okuyama, R. Nakayama, T. Kurino, (2008) MTSAT-1R Infrared Intercalibration on GSICS. **Proc CEReS Int. Symposium & SKYNET workshop**, Chiba University, Japan, Nov 2008.

Tobin, D., (2008) An SNO Analysis of IASI and AIRS Spectral Radiance, **GSICS Quarterly**, Vol.2, No.3.

Warren, S. G., (1984) Optical constants ofe ice from the ultraviolet to the microwave, **Applied Optics,** 23, 1206-1225.